International Journal of Automation and Computing 7(1), February 2010, 9-16
DOI: 10.1007/s11633-010-0009-7

# Interpolation of Images Using Discrete Wavelet Transform to Simulate Image Resizing as in Human Vision

Rohini S. Asamwar[1] Kishor M. Bhurchandi[1] Abhay S. Gandhi[2]

[1]Department of Electronics and Communication Engineering, Shri Ramdeobaba Kamla Nehru Engineering College, Nagpur 440013, India
[2]Department of Electronics and Computer Science, Visvesvaraya National Institute of Technology, Nagpur 440010, India

**Abstract:** This paper presents discrete wavelet transform (DWT) and its inverse (IDWT) with Haar wavelets as tools to compute the variable size interpolated versions of an image at optimum computational load. As a human observer moves closer to or farther from a scene, the retinal image of the scene zooms in or out, respectively. This zooming in or out can be modeled using variable scale interpolation. The paper proposes a novel way of applying DWT and IDWT in a piecewise manner by non-uniform down- or up-sampling of the images to achieve partially sampled versions of the images. The partially sampled versions are then aggregated to achieve the final variable scale interpolated images. The non-uniform down- or up-sampling here is a function of the required scale of interpolation. Appropriate zero padding is used to make the images suitable for the required non-uniform sampling and the subsequent interpolation to the required scale. The concept of zeroeth level DWT is introduced here, which works as the basis for interpolating the images to achieve bigger size than the original one. The main emphasis here is on the computation of variable size images at less computational load, without compromise of quality of images. The interpolated images to different sizes and the reconstructed images are benchmarked using the statistical parameters and visual comparison. It has been found that the proposed approach performs better as compared to bilinear and bicubic interpolation techniques.

**Keywords:** Discrete wavelet transform, non-uniform sampling, zeroeth level discrete wavelet transform (DWT), interpolation, human vision.

## 1 Introduction

When a human being observes any scene from a specific distance, a retinal image of that scene is generated on the retina of the observer. The retinal (at inner curved surface of human eyeball rear side) resolution is higher at the centre of the retinal plane within around a $6^{\circ}$ solid angle. However, the resolution is less in the peripheral regions[1]. This resolution depends on the eye (left or right), person, condition of the eye, illumination over the scene, wavelength of illumination, and many other factors. As far as this work is concerned, we consider the available original image as the retinal map obtained at the first instance by observing the scene.

However, the other parameters like illumination conditions, condition of the eye[2, 3] are neglected for simplicity, and of course, resolution is the current resolution of the image. As the observer moves towards the scene, the retinal image gets enhanced, and more details of the scene can be observed. On the other hand, if he/she moves away from the scene, the details are lost. Thus, to simulate movement towards the scene, the original image size needs to be increased, i.e., a bigger sized interpolated version of the scene needs to be computed. If the observer moves away from the scene, a lower resolution interpolated image needs to be computed. This paper presents such interpolations using Haar discrete wavelet transform. If the actual size of the object and distance from the observer are known, different interpolated versions for the changing distance between the human eye and the observer can be precisely computed.

Manuscript received March 10, 2009; revised May 31, 2009
This work was part of doctoral research work of Ms. Rohini S. Asamwar at Department of Electronics and Computer Science, Visvesvaraya National Institute of Technology, Nagpur, India.

A lot of work has already been done for interpolating the images using discrete wavelet transform. It was targeted at edges and texture enhancements such that after interpolation the smoothness of the visual images was maintained for photographic and printing purposes[4−13]. Comparatively, less emphasis was given on interpolation for the images of required size. Most of the algorithms were computationally heavy[6, 9, 10]. However, we could not come across any interpolation technique using discrete wavelet transform (DWT) which can predict the required image resizing factor in terms of DWT level, as proposed in this work.

During the last ten years, various interpolation techniques have been developed. Some of these techniques are wavelet-based interpolation techniques. Edge and texture enhancement scheme was presented in [4] using DWT in which images were handled as complete matrices and not piecewise and interpolation techniques were used to interpolate the edge pixels. Wavelet-based contour estimation in [5], which is again an edge enhancement approach, gave size variation only in multiple of power of 2. Wavelet fractal interpolation technique in [6] was a computationally complex method. For wavelet-based image interpolation using phase shift compensation, parametric modeling of probabilistic wavelet coefficients was required in [7].

Nonlinear models usually result in increased computational complexity. Interpolation using image resampling approach with neural network training and conversion was presented in [9], which is again a computationally complex method. Interpolation using wavelet-based hidden Markov trees results in image detail estimation[10]. For denoising applications, the hidden Markov model is useful, but for interpolation, the shortcoming is its inherent inability to

keep track of the sign of coefficients. Sampling and interpolation in [11] resulted in wavelet coefficients up to $n-1$, but coefficients at finer scale could not be computed. A thesis titled "mathematical techniques for image interpolation" presented edge-based correlation across sub-bands and gave out locally linear embedded (LLE) algorithm in which only zooming in technique was elaborated[12]. Some dynamically configurable vision and tracking systems were presented in [14, 15].

In this paper, we propose a simple algorithm for DWT-based variable-scale image interpolation. Conventional discrete wavelet transformation reduces the image size by a factor of $2^n$, n being an integer, whereas in this paper, it is proposed that image can be reduced to any (variable scale) size, using discrete wavelet transformation. Section 1 presents the outline of the paper and literature survey. Section 2 describes short outline of wavelet decomposition and reconstruction. In Section 3, similarity between human vision and DWT is discussed. Section 4 describes modification required to convert conventional DWT into (variable scale) piecewise DWT, followed by the same for inverse discrete wavelet transform (IDWT). The zeroeth level DWT concept is proposed in Section 5. Fractional level DWT concept is presented in Section 6. Comparison of the proposed method with other interpolation methods like bilinear and bicubic is presented in Section 7. Various parameters used to analyze the results are discussed in brief in Section 8 for variable scale interpolation. Conclusions is drawn in Section 9.

## 2 Discrete wavelet transform

DWT is a technique of decomposition of a complex signal in terms of its mother wavelet and is similar to the expansion of a function in the form of a series. The more the number of terms considered, the higher the accuracy. An image is a two-dimensional signal or a two-variable function. Hence, the series expansion is also two-dimensional.

The wavelet expansion at first level results in four images that provide sub-band information content of the image and are generated by appropriate sub-sampling and convolution with appropriate filter masks. The first level wavelet transformation gives four images, and they are low-pass followed by low-pass (LPLP-approximate details), low-pass followed by high-pass (LPHP-horizontal details), high-pass followed by low-pass (HPLP-vertical details), and high-pass followed by high-pass (HPHP-diagonal details)[16]. Hence, here the original image is reduced to a size equal to original size/4. Here, the number of rows and columns are reduced to half after the first level DWT application. Applying IDWT to the four DWT components yields the original image. For perfect reconstruction of an original image from these components, the filters must be perfectly reconstructable filters[17].

The finite resolution of digital machine and the approximations during computations result in reconstruction error. However, in general DWT is expected to retrieve more than 98 % energy of the original signal after reconstruction. Fig. 1 shows its schematic for wavelet implementation. The LPLP image is observed to be visibly similar to the original image but 50 % in dimension (resolution). Thus, it can be considered as a 50 % interpolated image.

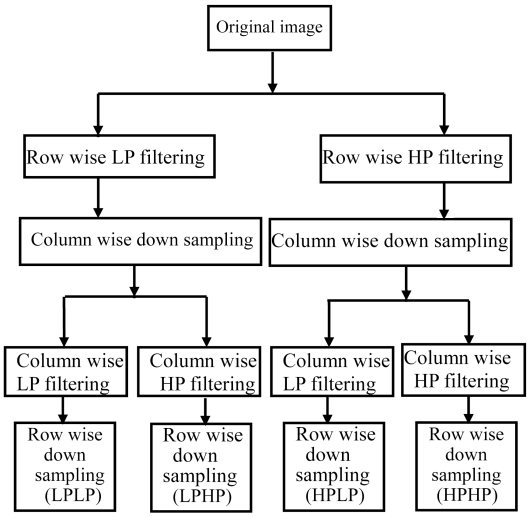


Fig. 1 Computation of DWT

## 3 Human vision and DWT

The proposed work plans to explore the relationship between the wavelet transform expansions of images and the analogous vision phenomenon. In most of the computer vision and image processing algorithms, it has been observed that even for executing simplest algorithms, the computing machines take a lot of time[18] and do not complete the task in real time. For example, to segment a given color image, even the fastest available machine may take much more time than that taken by a human being. Modern microprocessors have very high computational ability; they are suitable for completing repetitive tasks much faster than human brain.

However, the human brain is found to be faster than the computers for image processing and vision applications. It is possibly due to the massively parallel architecture of the human brain. This clearly indicates that the way of handling the vision data over the computing machines still requires a lot of research, and thus, the image processing and computer vision algorithms attract a sizable chunk of research efforts in this area. As pointed out earlier, the fact that computer vision and image processing algorithms take a lot of time for execution on high-speed machines as compared to human beings also further indicates the need of exploring the human visual system and orienting the computational algorithms according to the limitations and capabilities of human vision.

One example that can be cited here is an image directly taken from the camera. It may result in arbitrary number of segments as compared to a properly filtered and sampled image. As already stated above, the discrete wavelet transform refers to the multi-band decomposition of the given image. When a human being observes a particular scene, it also tends to remember the content of the scene or image in terms of four components. These components may be broadly described as low frequency components (segments in the image), i.e., LPLP, that are intermediate components in the image, and LPHP, HPLP, and HPHP components that represent high-frequency component (edges) in

the image.

Also, DWT can retrieve up to 98 % energy of original signal, and up to 2 % change in energy is not noticed by human eyes[19]. This fact roughly establishes similarity in the DWT and functioning of human vision. Another example that can be quoted is that, as the level of discrete wavelet transform goes on increasing, the LPLP result image appears to be the original image but viewed from a longer distance. This points to the fact that an object viewed from a longer distance appears to be smaller with fewer details, while the same object viewed from the smaller distance appears to be bigger with more detail, and this phenomenon may be modeled by appropriate level DWT.

## 4 Piecewise application of DWT

To model the movement of the observer, closer to and farther from the scene, initially, appropriate zero padding is done, followed by non-uniform sub-sampling and filtering, and then, DWT is applied in a piecewise manner. Finally, all the pieces of the DWT transformed signal are added to achieve the interpolated signal, which is described in Figs. 2 and 3.

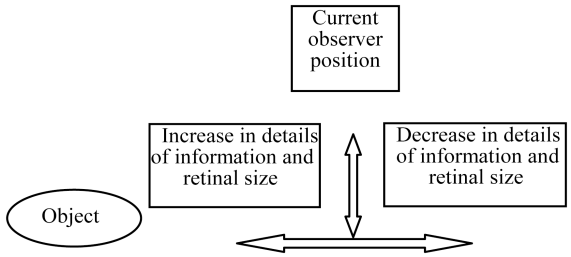


Fig. 2 Dependency of retinal/object size on movement of observer

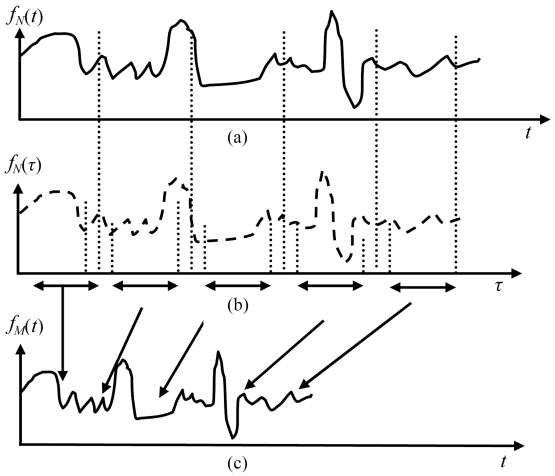


Fig. 3 Piecewise DWT processing on $f_N(t)$ to obtain $f_M(t)$. (a) Given one dimensional signal $f_N(t)$ for duration $t$; (b) $f_N(t)$ signal broken into pieces to obtain $f_N(\tau)$; (c) Piecewise processing of $f_M(\tau)$ to obtain $f_M(t)$

Fig. 2 shows that as the observer moves closer, the observed object size and retinal image size effectively increase, and if he moves farther from the object, the observed object size and the retinal image size effectively decrease. To model this, the available image is increased or decreased in its size and required interpolation is carried out. The DWT is applied in piecewise fashion to achieve this interpolation, as described below. As usual, DWT gives out 50 %, 25 %, and 12.5 % interpolation of the signal for the the first-, second-, and third- level DWT decomposition, but to achieve say 66 %, 75 %, or 33 % (or any odd scale) reduction using DWT, the proposed piecewise application of DWT is required. Similarly, 125 %, 150 %, or 200 % (or any odd scale) magnification using DWT can also be achieved using piecewise application of DWT. For that, the zeroeth level, $-$1st level, $-$2nd level, and $-n$-th level DWT are presented further.

**Algorithm for variable-scale interpolation.**

Let $f_N(t)$ be a band limited signal with $N$ samples. $f_N(t)$ is to be interpolated to a smaller size with $M$ samples $f_M(t)$. Obviously, $M < N$, or the resulting signal $f_M(t)$ will be having $(N - M)$ less samples than $f_N(t)$. These $(N - M)$ samples will be dropped from $f_N(t)$ uniformly all over $f_N(t)$ such that no two or more neighbouring samples are dropped due to down-sampling, i.e., only one sample can be dropped in each specified window. This is possible only if $N/n = N - M$, where $n$ is the nonzero positive smallest integer satisfying the above equality. If $N/n \neq N - M$, then $N$ is incremented by zero padding to $N'$ so that $N'/n = N - M$. Let the number of samples of $f_N(t)$, $N = 100$, and the required interpolated signal samples of $f_M(t)$, $M = 67$, i.e., a 33 % reduction. Therefore, the number of samples to be dropped is $N-M = 100-67 = 33$. Now, $N/n = 100/3 = 33.333$. Thus, $N-M \neq N/n$. Hence, zero padding is needed. The number of samples to be zero padded can be computed as $N' = N + z = 100 + 2 = 102$. Now, $N'/n = 102/3 = 34 \approx 33$.

Other alternative is to drop the last $|(N/n)|$ samples, i.e., in the above case, last $|(N/n)| = 1$ sample will be dropped. However, it is to be noted that such dropping of samples results in loss of information corresponding to the dropped columns. Hence, the earlier technique is preferred. Now, the signal $f_N(t)$ is windowed using a train of pulses as follows:

$$\sum u_p(n')|_{p=1:(N-M)}^{n'=1:n} = 1. \tag{1}$$

The resulting signal can be expressed as

$$f_N(\tau) = f_N(t) \sum u_p(n') \,|_{p=1:(N-M)}^{n'=1:n} = \sum f_N(t) u_p(n') \,|_{p=1:(N-M)}^{n'=1:n} . \tag{2}$$

Therefore, if DWT stands for piecewise DWT, we have

$$\mathrm{DWT}(f_N(\tau)) = \mathrm{DWT}(\sum f_N(t) u_p(n') \,|_{p=1:(N-M)}^{n'=1:n}). \tag{3}$$

As DWT is an associative transform, (3) is bound to be valid.

$$\mathrm{DWT}[f_N(t) u_p(n') \,|_{p=1:(N-M)}^{n=1:n}] = \mathrm{DWT}[f_p(n')]. \tag{4}$$

where $f_p(n') = f_N(t) u_p(n') \,|_{n'=1:n}$.

DWT of $f_p(n')$ can now be computed in a piecewise manner as shown below. The low pass filter is applied. This signal is divided into pieces of $n$ samples each. Then, out of every $n$ samples, one sample $n' = 1 : n$ is dropped at a time, and we get $f_p(n' - 1)$. Thus, for each $n'$ sample interval by changing $n'$ to $1 : n$, we get $n$ samples of

$f_p n'(n-1)$. By adding all $f_p n'(n-1)$, we get $f_p(n-1)$ for each $p = 1 : N - M$. This is the proposed non-uniform down-sampling. Thus, for all $p$, total $(N - M) = p$ samples will be dropped, reducing the size of $f_N(t)$ to $f_M(t)$. Thus, all $f_p(n-1)$ will be added to obtain $f_M(t)$, i.e., coarse portion of DWT (LPLP), as shown in Fig. 4.

A high pass filter applied in the same manner yields the details. In case of images, this algorithm will be first applied row-wise and then column-wise. The above algorithm actually interpolated the size of the available image to the required smaller size in the form of coarse part of the DWT of $f_N(t)$. While the remaining three parts are also computed using similar down-sampling over $n' = 1 : n$ for all $p$ and then adding all the resulting $M$ size vectors to obtain $f_M(t)$ in both directions. The four parts of DWT can be used for reconstruction.

For increasing the given size of $f_N(t)$ to $f_M(t)$, where $M > N$, zero padding is done to increase $N$ to $N'$ so that $z$ samples are inserted at the end of $f_N(t)$ to make $N'$ integral multiple of $p = (M - N')$. Let $n = N'/(M - N)$, and further, $f_{N'}(t)$ is inserted with zero samples uniformly such that in each $n$ samples one zero sample is inserted. This is the proposed non-uniform up-sampling followed by LP and HP filter application as in IDWT to obtain a vector $f_p(n+1)$ for all $p = 1 : (M - N)$ and for all $n' = 1 : n$. $f_M(t)$ is obtained on summation of all $f_p(n')$ as

$$f_M(t) = \sum_{p=1}^{p=(M-N)} f_p(n'). \tag{5}$$

This is the piecewise application of DWT algorithm.

For application to images, the same procedure is applied row wise and then column wise as in Fig. 5. Thus, piecewise application of DWT with appropriate zero padding yields reduction to the required size, while piecewise application of IDWT with appropriate zero padding yields increase to the required size. The interpolations for $M < N$ and $M > N$ are carried out followed by the reconstructions. The mean squared error (MSE), peak signal to noise ratio (PSNR), and qualitative statistical measures based on human visual information are presented along with the result images in the result section.

## 5 Zeroeth level DWT

In conventional DWT, the 1st level, 2nd level, and 3rd level image decompositions and the corresponding LPLP components resize the image to 50 %, 25 %, and 12.5 % of the original image size. Thus, the conventional DWT will provide only reduction of image size that takes place when one moves away from the object/scene. For providing magnification of the scene/image when one moves closer to the

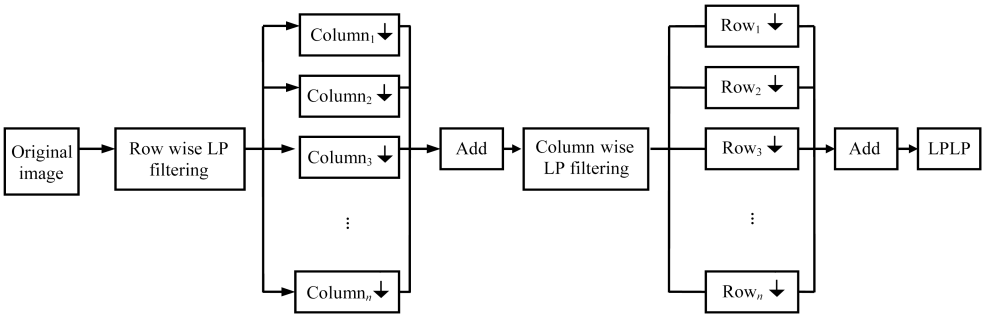


Fig. 4 Schematic for piecewise application of DWT

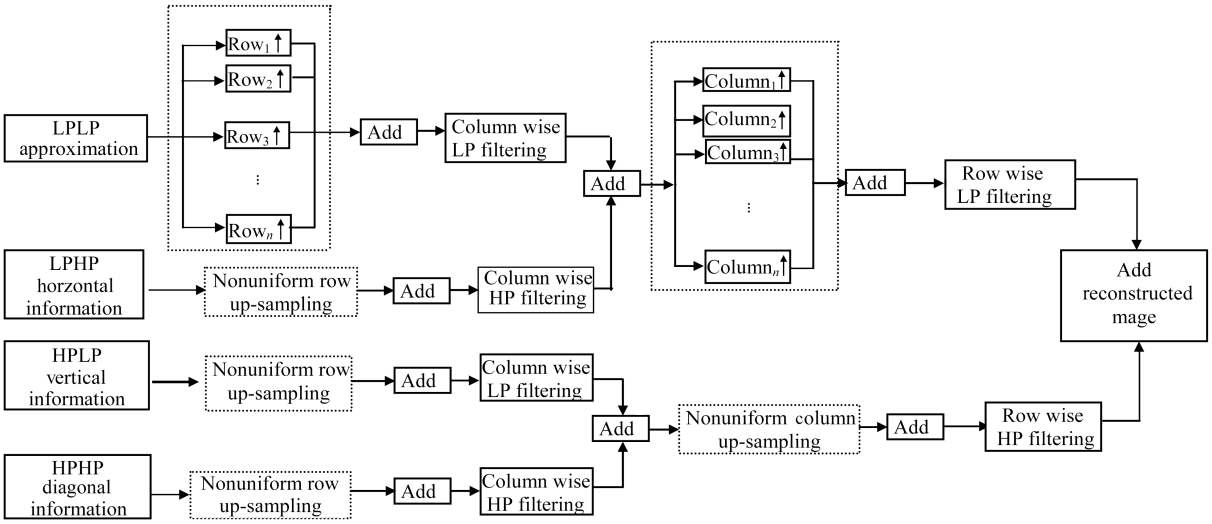


Fig. 5 Schematic for piecewise application of IDWT

object/scene, the conventional discrete wavelet transform does not provide any technique. We have presented the zeroeth level DWT of an image to generate the four sub-band images from the original image at the same scale, and it is the first step to interpolate the image to the bigger sizes than the original one. The zeroeth level DWT images are presented in the result section, containing original image, zeroeth level LPLP, LPHP, HPLP, and HPHP components. Algorithm for the zeroeth level DWT is presented further.

**Algorithm for zeroeth level DWT.**

Let $H$ be the low pass filter and $G$ be the high pass filter. Then, the algorithm for the zeroeth level DWT can be given in a stepwise manner as follows:

**Step 1.** Signal $f(x, y)$ is convolved with the low pass filter $H$ row-wise to obtain low-pass (LP) version of that signal $f(x, y)_{\mathrm{LP}}$.

**Step 2.** The obtained signal $f(x, y)_{\mathrm{LP}}$ is once again convolved with the low pass filter column-wise to obtain low-pass low-pass (LPLP) version of the image. Thus, (without down-sampling as in conventional DWT) LPLP component of the zeroeth level DWT is obtained and is denoted by $f(x, y)_{\mathrm{LPLP}}$.

**Step 3.** The low pass version of the image $f(x, y)_{\mathrm{LP}}$ is convolved with high pass filter $G$ to obtain low-pass high-pass version (LPHP) of the image $f(x, y)_{\mathrm{LPHP}}$, which relates to LPHP component of conventional DWT but obtained here without down-sampling of the original signal.

**Step 4.** Similar procedure is adopted to obtain the zeroeth level HPLP and HPHP components of the image.

IDWT procedure can be successively applied to these four components to obtain bigger size interpolated version of the given image. Further continuing the application of the IDWT, the −1st level, −2nd level, and −3rd level IDWT can be computed. Thus, continued application of the zeroeth level DWT algorithm followed by IDWT can yield magnification of the image size.

## 6 Fractional level DWT

Conventional DWT interpolates the image size by a factor $2^n$, where $n$ is an integer. In other words, it reduces the image size by the above said factor. To interpolate a given image to any odd size other than $2^n$, where $n > 0$; obviously, fractional level DWT will be required. Therefore, to increase the image size, the zeroeth level DWT is carried out, as already explained in Section 5. Further, the −1st level, −2nd level, −3rd level, etc., can be worked out to achieve magnification of the image to 200 %, 400 %, 800 %, and so on corresponding to the conventional DWT processing. Again, to interpolate the size of the given image to any odd size other than $2^n$, where $n < 0$, the fractional level DWT will be required.

The fractional level DWT is implemented by applying the conventional DWT in a piecewise manner to achieve any odd scale (fractional level) DWT. The graph can be plotted for level of DWT against decrease in size of the image. Similarly, the zeroeth level DWT and further the −1st level, −2nd level, and −3rd level DWT can yield magnification of the image. These can further be plotted for level of DWT against change in image size to yield the plot, as shown in Fig. 6. For example, suppose if interpolation of given image is required to size 67 %, that is, there will be a reduction of 33 %. The order of the DWT $n$ is such that $0 < n < 1$. The resulting image will be 67 % of the original image as already discussed. When $n = 1$, interpolation to size 50 % will be achieved using first level DWT. Suppose the interpolation is expected to reduce the image to 33 %, the required order of DWT $n > 1$. Here, the resulting image will be 33 % in size.

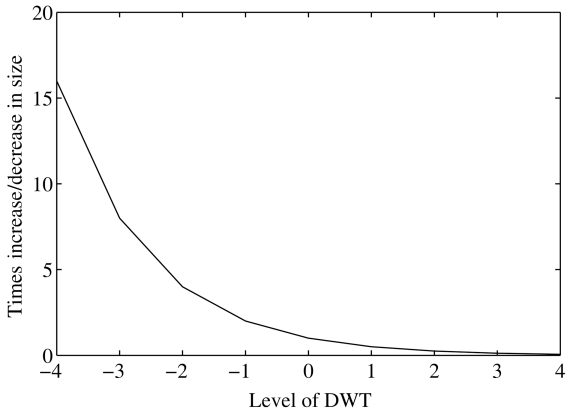


Fig. 6 Size variations against level of DWT

This can be achieved by splitting the percentage 67% = 50%+17%. Further, 50 % reduction is achieved using DWT ($n = 1$). The remaining 67% − 50% = 17% reduction can now be thought of as 34 % of the already 50 % reduced image using DWT ($n = 1$) and can be implemented further. Similarly, 78 % reduction can be achieved using DWT with $n = 2$, yielding 75 % reduction and resulting in 25 % size of the original image. The remaining 78 − 75 = 3% reduction can be thought of as $3 \times 2^n = 12\%$ of the existing 25 % size. Similarly, if 140 % increase in size is required, then first the zeroeth level DWT needs to be computed as already discussed, followed by DWT with $n = -1$ (IDWT), yielding 100 % rise in size. The remaining 40 % rise can be considered as 20 % of the resulting image and can subsequently be computed. Thus, the fractional level DWT has been implemented, and any odd size interpolation can be achieved. It is to be noted here that the computational load for interpolating the given image to a different scale also varies depending upon the factor of reduction or magnification.

## 7 Comparison of various methods

As DWT interpolates the image size by a factor $2^n$ where $n$ is an integer, it is considered here as a tool to interpolate the image to simulate interpolation like human vision. Here, DWT based interpolation method is compared with traditional bilinear and bicubic interpolation methods. The 1st level, 2nd level, and 3rd level DWT reduce the image to 50 %, 25 %, 12.5 %, and so on (accordingly the image area reduces to $2^2$, $2^4$, and $2^6$ times of the original image area). Corresponding reduction in size is experimented with bilinear and bicubic interpolation methods and subsequent reconstructions. In fact, we have experimented up to 10 levels of DWT.

However, the DWT results are presented here only up to the 4th level. After the 6th level, the reconstruction error or MSE is found to increase gradually, and the image

also starts degrading visibly. For this experimentation, the values of MSE and PSNR are compared. In fact, several interpolation experiments were carried out on a large number of images. All those images were magnified, as well as reduced, and every time, the reconstruction error was computed. However, the values of MSE for 50 %, 25 %, 12.5 %, and 6.25% reduction and the subsequent reconstruction error for bilinear, bicubic, and DWT interpolation methods for some of them are presented in Table 1.

The values of MSE of DWT-based interpolation method are found better as compared to bilinear and bicubic interpolation in most of the cases. For the 1st level DWT interpolation, the MSE values are found to be comparable to the corresponding reduction in few cases of bicubic interpolation technique. For the 2nd level DWT interpolation, the values of MSE obtained are better as compared to corresponding results of bicubic interpolation. Thus, exhibiting its best performance for 25% reduction in size, DWT is found to be the best interpolation method when compared with the other two.

Similarly, at the 3rd and 4th levels, i.e., for reductions in size to 12.5 %, 6.25 %, and so on, the DWT interpolation method can be considered as the best interpolation method. The above three methods of interpolation were studied for six different tagged image file (TIF) format images, and corresponding MSE values are tabulated in Table 1. Graphically, these three methods can be compared for their corresponding values of MSE for various percentage reductions in size and are plotted here in Fig. 7 for the cameraman image. As already said, after the 6th level of DWT (image area reduction to $2^{2n}$, i.e., $2^{12} = 4$k times the original image), the reconstruction introduces considerable error (MSE), and the images become somewhat visibly distorted. After the 10th level of DWT (image area reduction to $2^{20}$= 1M times the original image size), the results are visibly unacceptable. Fig. 8 shows the comparative performances for 25% reduction in size for bilinear, bicubic, and DWT based interpolations.

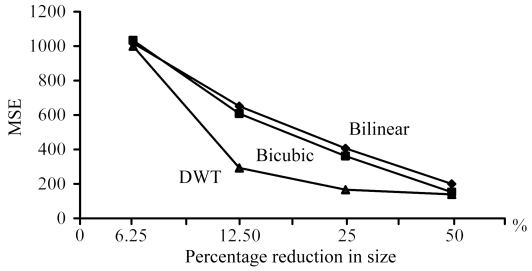


Fig. 7 MSE versus percentage reduction in size for bilinear, bicubic, and DWT interpolations

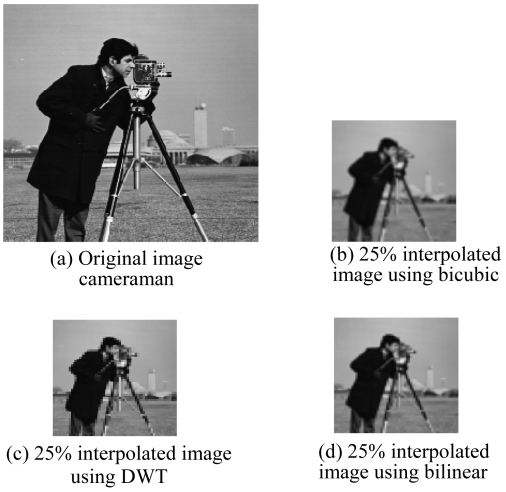


Fig. 8 Comparative performances for 25% reduction in size for bilinear, bicubic, and DWT-based interpolations

## 8 Results

To evaluate the performance of the interpolation scheme quantitatively, PSNR and MSE have been calculated. The MSE is defined as

$$\text{MSE} = \frac{1}{m \times n} \sum_{i=1}^{m} \sum_{j=1}^{n} (x_{ij} - y_{ij})^2 \tag{6}$$

where $m$ and $n$ are the numbers of rows and columns, respectively. $x_{ij}$ and $y_{ij}$ denote the original and reconstructed signals, respectively, where $i = 1 : m$ and $j = 1 : n$.

The PSNR is defined as

$$\text{PSNR} = 20 \log_{10} \frac{255}{\sqrt{MSE}}. \tag{7}$$

The proposed interpolation method and other popular existing interpolation approaches are compared in this study. Thus, we compared three interpolation methods: the 2-dimensional bidirectional linear interpolation (denoted by "bilinear"), the cubic interpolation (denoted by "bicubic"), and the proposed piecewise DWT interpolation scheme in the simulations. Table 2 shows the MSE and PSNR values (dB) of the simulation results for the reconstructed still images. The images were shown to more than 100 observers, and they were requested to discriminate between original and reconstructed images. The percentage of matching by the observers has been presented as picture reconstruction quality by human observer on the same lines of picture quality and structural similarity by human observers[20, 21].

Table 1 Comparison of bilinear, bicubic, and DWT interpolation MSE values for various TIF images

| Image | 50 % reduction | | | 25 % reduction | | | 12.5 % reduction | | | 6.25 % reduction | | |
|---|---|---|---|---|---|---|---|---|---|---|---|---|
| | Bilinear | Bicubic | DWT | Bilinear | Bicubic | DWT | Bilinear | Bicubic | DWT | Bilinear | Bicubic | DWT |
| Cameraman | 200 | 152 | 140 | 407 | 361 | 166 | 651 | 608 | 293 | 1017 | 1033 | 1000 |
| Circuit | 26 | 13 | 31 | 110 | 90 | 39 | 241 | 220 | 184 | 554 | 552 | 457 |
| Pout | 6 | 4 | 19 | 25 | 19 | 10 | 60 | 52 | 36 | 123 | 120 | 100 |
| Airplane | 66 | 52 | 102 | 147 | 132 | 177 | 228 | 222 | 74 | 319 | 318 | 250 |
| Fishing boat | 91 | 66 | 67 | 215 | 187 | 63 | 363 | 343 | 165 | 589 | 585 | 545 |
| Pentagon | 94 | 73 | 100 | 167 | 151 | 103 | 246 | 231 | 90 | 378 | 379 | 302 |

Figs. 9 and 10 show the original size of airplane and pentagon images along with their 66% interpolated size, respectively. Fig. 11 shows various DWT components for piecewise application of DWT for 66 % interpolation of a circuit image. Fig. 12 shows the four zeroeth level components of the image. To construct the image of bigger size, the four components will be subjected to the non uniform up-sampling and the piecewise IDWT procedure after the zeroeth level DWT.

Table 2 Various TIF images showing their MSE and PSNR values for 66 % interpolated size for bilinear, bicubic and Haar DWT

| Image | MSE | | | PSNR (dB) | | | Picture quality |
|---|---|---|---|---|---|---|---|
| | Bilinear | Bicubic | Haar DWT | Bilinear | Bicubic | Haar DWT | Human observers |
| Airplane | 159 | 49 | 34 | 31 | 32 | 26 | 99 % |
| Pentagon | 233 | 150 | 117 | 26 | 27 | 24 | 100 % |
| Pout | 17 | 5 | 4 | 40 | 41 | 35 | 98 % |
| Circuit | 51 | 19 | 8 | 35 | 38 | 31 | 99 % |
| Tank | 113 | 170 | 648 | 25 | 20 | 27 | 98 % |
| Boat | 51 | 58 | 55 | 30 | 30 | 30 | 99 % |

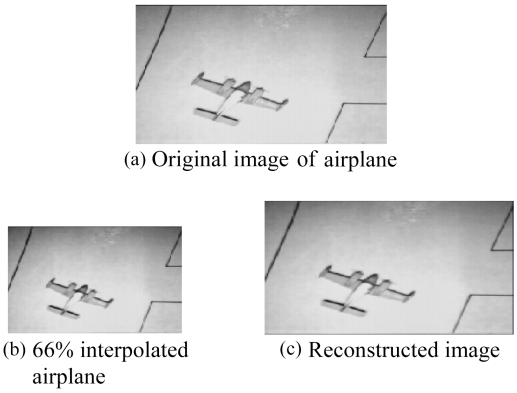


Fig. 9 Original image of airplane, 66 % interpolated airplane, and reconstructed image

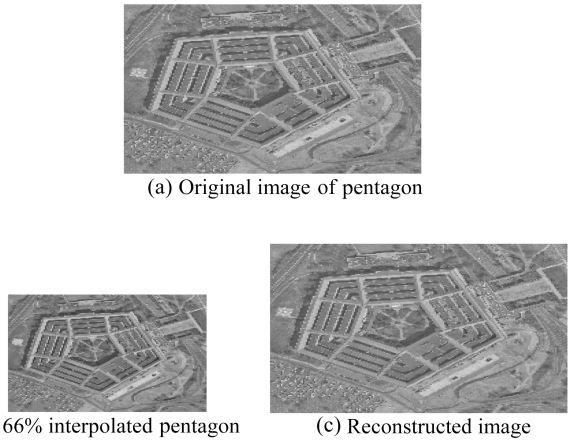


Fig. 10 Original image of pentagon, 66 % interpolated pentagon, and reconstructed image

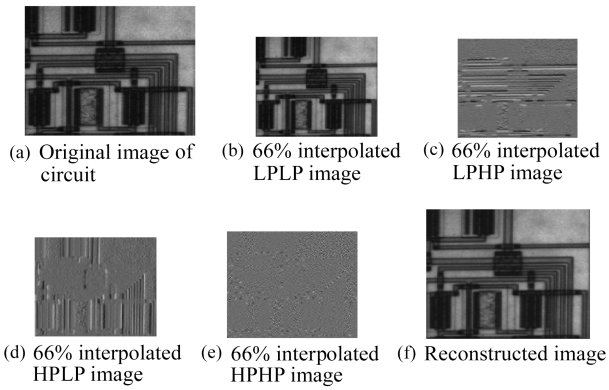


Fig. 11 Circuit image showing DWT components (LPLP, LPHP, HPLP, and HPHP) for 66 % interpolation using piecewise application of DWT

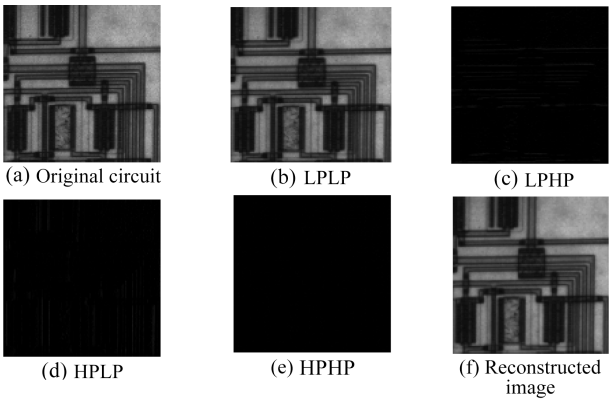


Fig. 12 Circuit, zeroeth level DWT components of circuit and reconstructed image

## 9 Conclusions

The DWT-based interpolation method is compared with bilinear and bicubic interpolation methods. A scheme of interpolation of images to varying sizes using piece-wise application of DWT and IDWT has been presented along with its quantitative results. The discrete Haar wavelet with two elements has been found to yield results comparable to bilinear and bicubic interpolation techniques but at a much less computational load. The important point is that no visual distortion is observed in the reconstructed images.

Better MSEs and PSNRs can be achieved using higher size wavelet approximations like Daubechies, but computational load may increase tremendously.

The concept of the zeroeth and $-n$-th level DWT has been introduced, which leads to magnification of images using piece-wise inverse Haar discrete wavelet computations. The comparable MSE, PSNR, and low visible distortion at a less computational load makes this scheme more suitable for vision applications. We have experimented up to 10 levels of DWT. DWT results up to the 4th level, and its corresponding comparison with other two methods are presented in this paper. Gradual increase in MSE is found after reconstruction from the 6th level DWT. The results are visibly unacceptable after 10th level of DWT. The 10th level DWT

results in $2^{10}$ times reduction in each image dimension or $2^{20}$ times reduction in the number of image pixels.

## References


[1] A. C. Guyton. *Textbook of Medical Physiology*, 10th ed., Philadelphia, USA: W. B. Saunders Company, pp. 784–824, 2000.

[2] G. Nussbaum. The retina as a two-dimensional detector array in the context of color vision theories and signal detection theory. *Proceedings of the IEEE*, vol. 69, no. 7, pp. 772–786, 1981.

[3] G. Buchsbaum. An analytical derivation of visual nonlinearity. *IEEE Transactions on Biomedical Engineering*, vol. BME-27, no. 5, pp. 237–242, 1980.

[4] S. H. G. Chang. Image Interpolation Using Wavelet Based Edge Enhancement and Texture Analysis, Technical Report UCB/ERL M95/100, Master dissertation, Electrical Engineering and Computer Science, University of California, Berkeley, USA, 1995.

[5] H. F. Ates, M. T. Orchard. Image interpolation using wavelet-based contour estimation. In *Proceedings of IEEE International Conference on Acoustics, Speech, and Signal Processing*, IEEE, vol. 3, pp. 109–112, 2003.

[6] G. F. Tu, C. Zhang, J. K. Wu, X. Z. Liu. Remote sensing image processing using wavelet fractal interpolation. In *Proceedings of International Conference on Communications, Circuits and Systems*, IEEE, vol. 2, pp. 701–706, 2005.

[7] S. S. Kim, I. K. Eom, Y. S. Kim. Wavelet based image interpolation using phase shift compensation. In *Proceedings of the 7th IEEE Workshop on Multimedia Signal Processing*, IEEE, pp. 1–4, 2005.

[8] P. E. Barrett, L. L. Dressel. Spectral extraction of extended sources using wavelet interpolation. In *Proceedings of HST Calibration Workshop*, Space Telescope Science Institute, USA, pp. 260–266, 2005.

[9] Y. L. Huang. Wavelet based image interpolation using multilayer perceptrons. *Neural Computing & Applications*, vol. 14, no. 1, pp. 1–10, 2004.

[10] K. Kinebuchi, D. D. Muresan, T. W. Parks. Image interpolation using wavelet based hidden Markov trees. In *Proceedings of IEEE International Conference on Acoustics, Speech and Signal Processing*, IEEE, Salt Lake City, UT, USA, vol. 3, pp. 1957–1960, 2001.

[11] D. L. Donoho. Interpolating Wavelet Transforms, Technical Report, Department of Statistics, Stanford University, USA, 1992.

[12] T. Wittman. Mathematical Techniques for Image Interpolation, Report Submitted for Completion of Mathematics Department Oral Exam, Department of Mathematics, University of Minnesota, USA, 2005.

[13] E. Dumic, S. Grgic, M. Grgic. The use of wavelets in image interpolation: Possibilities and limitations. *Radioengineering*, vol. 16, no. 4, pp. 101–109, 2007.

[14] A. De Cabrol, T. Garcia, P. Bannin, M. Chetto. A concept of dynamically reconfigurable real time vision system for autonomous mobile robotics. *International Journal of Automation and Computing*, vol. 5, no. 2, pp. 174–184, 2008.

[15] M. M. Zhang, Z. G. Pan, L. F. Ren, P. Wang. Image based virtual exhibit and its extension to 3D. *International Journal of Automation and Computing*, vol. 4, no. 1, pp. 18–24, 2007.

[16] R. C. Gonzalez, R. E. Woods, S. L. Eddins. *Digital Image Processing Using MATLAB*, First India Print, Delhi, India: Pearson Education (Singapore) Pte. Ltd., Indian Branch Delhi, 2004.

[17] M. Vetterli, J. Kovacevic. *Wavelets and Subband Coding*, Englewood Cliffs, New Jersy, USA: Prentice Hall PTR, 1995.

[18] A. K. Jain. *Fundamentals of Digital Image Processing*, New Jersy, USA: PHI Press, 1989.

[19] P. Kaufman, A. Alm. *Adler' Physiology of the Human Eye*, USA: Jaypee Brothers, pp. 708, 1989.

[20] M. Miyahara., K. Kotani, V. R. Algazi. Objective picture quality scale (PQS) for image coding. *IEEE Transactions on Communications*, vol. 46, no. 9, pp. 1215–1226, 1998.

[21] Z. Wang, A. C. Bovik, H. R. Sheikh, E. P. Simoncelli. Image quality assessment: From error visibility to structural similarity. *IEEE Transactions on Image Processing*, vol. 13, no. 4, pp. 600–612, 2004.



**Rohini S. Asamwar** received the B. Eng. degree in electronics and teleommunication in 1999 from Shri Sant Gajanan Maharaj College of Engineering (SSGMCE), Shegaon (Amravati University), India. She received the M. Tech. degree in electronics engineering from Yeshvantrao Chavan College of Engineering, Nagpur, India in 2005. After working for four years as a faculty member, she joined Shri Ramdeobaba Kamla Nehru Engineering College, Nagpur, India as a lecturer in July 2003. After registering for Ph. D. in July 2006, she is carrying out her doctoral research work at Visvesvaraya National Institute of Technology (VNIT, formerly VRCE), Nagpur, India. She is a member of ISTE and IAENG.

Her research interests include communication engineering and image processing.

E-mail: rohini_asamwar@rediffmail.com (Corresponding author)



**Kishor M. Bhurchandi** received the B. Eng. and M. Eng. degrees in electronics engineering from Shri Guru Gobind Singhji College of Engineering and Technology, Nanded, India in 1990 and 1992. He received the Ph. D. degree from Visvesvaraya Regional College of Engineering, Nagpur (recently known as VNIT, Nagpur) under Nagpur University, India in 2004. Currently, he is a professor in the Department of Electronics and Communication Engineering at Shri Ramdeobaba Kamla Nehru Engineering College, Nagpur, India. He has coauthored a book titled *Advanced Microprocessors and Peripherals published* by McGraw Hill. He has contributed a chapter on Color Image Processing to a book titled *Information Technology* authored by A. K. Ray and Tinku Acharya and published by PHI. He has also filed an Indian patent application for on line monitoring of energy meters using telephone lines. He is member of professional societies like IEEE, IE, ISTE, and IUPRAI.

His research interests include pattern recognition, image and video processing, computer vision, biologically inspired image processing and computer vision, wavelet transform, and very large scale integration (VLSI) architectures for signal processing.

E-mail: bhurchandikm@rknec.edu


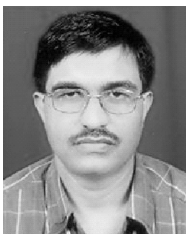


**Abhay S. Gandhi** received the B. Eng. degree in electronic engineering from Visvesvaraya Regional College of Engineering (VRCE), Nagpur (Nagpur University), India in 1989. He received the M. Eng. degree in electrical communication engineering from the Indian Institute of Science, Bangalore, India in 1991. After working for three years in industry and teaching, he joined Visvesvaraya National Institute of Technology (VNIT, formerly VRCE), as lecturer in July 1994. He received the Ph. D. degree from Nagpur University in 2002. He is a member of IETE and ISTE.

His research interests include signal processing, wireless digital communication, radio frequency (RF) circuits, and computer networks.

E-mail: asgandhi@ece.vnit.ac.in